Modelling dynamics of amperometric biosensors in batch and flow injection analysis

R. Baronas [a], F. Ivanauskas [a,b] and J. Kulys [c]

[a] *Faculty of Mathematics and Informatics, Vilnius University, Naugarduko 24, 2600 Vilnius, Lithuania*
E-mail: romas.baronas@maf.vu.lt
[b] *Institute of Mathematics and Informatics, Akademijos 4, 2600 Vilnius, Lithuania*
E-mail: feliksas.ivanauskas@maf.vu.lt
[c] *Institute of Biochemistry, Mokslininku 12, 2600 Vilnius, Lithuania*
E-mail: jkulys@bchi.lt

A mathematical model of amperometric biosensors has been developed. The model is based on non-stationary diffusion equations containing a non-linear term related to Michaelis–Menten kinetic of the enzymatic reaction. Using digital simulation, the influence of the substrate concentration as well as maximal enzymatic rate on the biosensor response was investigated. The digital simulation was carried out using the finite difference technique. The model describes the biosensor action in batch and flow injection regimes.

KEY WORDS: reaction-diffusion, modelling, biosensor, flow injection

AMS subject classification: 35K57, 65M06, 76R50, 92C45.

1. Introduction

Biosensors are devices that combine the selectivity and specificity of a biologically active compound with a signal transducer and an electronic amplifier [1–3]. The transducer converts the physico-chemical change of the biological sensing element, usually an enzyme, resulting from the interaction with analyte into an output concentration dependent signal. The biosensors are classified according to the nature of the physical transducer. The amperometric biosensors measure the changes of the current on a working indicator electrode due to direct oxidation of the products of the biochemical reaction [2–4]. In this case the potential at the electrode is held constant while the current flow is measured. The amperometric biosensors are known to be reliable, cheaper and highly sensitive for environment, clinical and industrial purposes.

Starting from the publication of Clark and Lyons [1], the amperometric biosensors became one of the popular and perspective trends of biosensorics [2]. The understanding of the kinetic regularities of the biosensors is of crucial importance for their design. The general features of amperometric response was analyzed in the publications of Mell and Maloy [5,6]. However, due to limiting calculation possibilities and unperfect mathematics, the calculations were restricted by two critical concentrations of

substrate when enzyme acted at the first- and zero-order reaction conditions. Some later reports were also devoted to calculate steady-state and non-stationary kinetics of amperometric biosensor response [7–11]. The development the numerical methods of solving of partial differential equations and facilities of modern computers open possibilities to make calculation at all interval of substrates concentration and at different diffusion and enzymatic reaction rate. The goal of this investigation is to make a model allowing an effective computer simulation of membrane biosensor as well as to investigate the influence of the kinetic parameters on the response of the biosensors. The developed model is based on non-stationary diffusion equations [12], containing a non-linear term related to the enzymatic reaction. The model allows to simulate the biosensor action in batch and flow injection regimes. In the flow injection analysis the biosensor contacts with the substrate for short time whereas in the batch analysis the biosensor is assumed as immersed in the substrate solution of infinite volume and during long time [13].

In this paper, digital simulation of the biosensor response was carried out using the implicit finite difference scheme [14,15]. The explicit scheme is usually easier to program, however, the implicit scheme has a higher simulation speed [8,10,15–17]. The developed program was employed also to generate multiple biosensor response data for four specific analytes of various concentrations. The generated data was used for the amperometric calibration of a biosensor array. Development of methods of analysis of mixtures with a biosensor array and chemometrics using a non-linear multivariate calibration is following [18,19]. The software for characterisation of wastewater (alarm system) is under development.

2.   Mathematical model

During an enzyme-catalyzed reaction

$$S \xrightarrow{\text{E}} P \tag{1}$$

the substrate (S) binds to the enzyme (E) to form enzyme-substrate complex. While it is a part of this complex, the substrate is converted to product (P). The rate of the appearance of the product depends on the concentration of the substrate.

In the simplest case, when the diffusion of substrate molecules is neglected and steady-state conditions are assumed for the enzyme reaction, the mathematical model of enzyme kinetics is given by Michaelis–Menten equation:

$$v = \frac{\mathrm{d}P}{\mathrm{d}t} = -\frac{\mathrm{d}S}{\mathrm{d}t} = \frac{V_{\max}S}{K_{\mathrm{M}} + S}, \tag{2}$$

where v is the rate of the enzymatic reaction, $V_{\max}$ is the maximal enzymatic rate attainable with that amount of enzyme, when the enzyme is fully saturated with substrate, K_{M} is the Michaelis constant, S is the substrate concentration, P is concentration of the reaction product, and t is time. $V_{\max}$ corresponds to relative activity of substrate.

Let us consider a membrane amperometric biosensor which can be treated as enzyme electrode, having a layer of enzyme immobilized onto the surface of the probe. The Michaelis–Menten model (2) of enzyme kinetics describes the steady-state kinetics of biosensors satisfactorily when the rate of enzyme conversions exceeds the rate of mass transfer [2]. However, the mass transfer by diffusion is a first-order reaction with respect to substrate concentration [8]. Imposing a diffusion thus has the effect of extending the linear range of initial reaction velocity beyond the K_M in (2) value of the normal enzyme. Because of this linear relationship, however, the observed rate of the reaction, and therefore analytical signal, is lower than would have been in a kinetically controlled enzyme reaction conforming to the rectangular hyperbola of Michaelis–Menten kinetics.

Let us assume the symmetrical geometry of the electrode and homogeneous distribution of immobilized enzyme in the enzyme membrane. Considering one-dimensional diffusion, coupling of reaction (1) with the diffusion described by Fick's law leads to the following equations:

$$\frac{\partial S}{\partial t} = D_S \frac{\partial^2 S}{\partial x^2} - \frac{V_{max} S}{K_M + S}, \quad 0 < x < d, 0 < t \leqslant T, \tag{3}$$

$$\frac{\partial P}{\partial t} = D_P \frac{\partial^2 P}{\partial x^2} + \frac{V_{max} S}{K_M + S}, \quad 0 < x < d, 0 < t \leqslant T, \tag{4}$$

where d is thickness of enzyme layer, T is full time of biosensor operation to be analyzed, D_S and D_P are diffusion coefficients of the substrate and product, respectively.

The operation of biosensor starts when some substrate appears over the surface of the enzyme layer. This is used in the initial conditions ($t = 0$)

$$S(x, 0) = 0, \quad 0 \leqslant x < d, \qquad S(d, 0) = S_0, \tag{5}$$

$$P(x, 0) = 0, \quad 0 \leqslant x \leqslant d, \tag{6}$$

where S_0 is the concentration of substrate (bulk) over the biosensor.

Because of electrode polarization, the concentration of the reaction product at the electrode surface is being permanently reduced to zero. If the substrate is well-stirred and in powerful motion, then the diffusion layer ($0 < x < d$) will remain at a constant thickness. Consequently, the concentration of substrate as well as product over the enzyme surface (bulk solution/membrane interface) remains constant while the biosensor contacts with the substrate. In the flow injection regime the biosensor contacts the substrate for short time only (seconds to tens of seconds) [13]. When the analyte disappears, a buffer solution swills the enzyme surface, reducing the substrate concentration at this surface to zero. Because of substrate (analyte) remaining in the enzyme membrane, the mass diffusion as well as the reaction still continues some time even after the disconnect of the biosensor and substrate. This is used in the boundary conditions ($0 < t \leqslant T$) given by

$$\left. \frac{\partial S}{\partial x} \right|_{x=0} = 0, \tag{7}$$

$$S(d, t) = \begin{cases} S_0, & t \leqslant T_F, \\ 0, & t > T_F, \end{cases} \tag{8}$$

$$P(0, t) = P(d, t) = 0, \tag{9}$$

where T_F is the time of flow injection, i.e., the time when analyte disappears from the bulk solution/membrane interface.

In the batch regime of the analysis the modelled biosensor remains as immersed in the substrate all the analyzing time. Assuming $T_F = T$ the model expressed by equations (3)–(9) may be accepted for batch analysis as well. In the batch analysis the boundary condition (8) reduces to $S(d, t) = S_0, t \leqslant T$.

3. Digital simulation

Definite problems arise when solving analytically the non-linear partial differential equations with complex boundary conditions [12,15]. To obtain an approximate analytical solution, approximation and classification of each different condition are needed. On the other hand, digital simulation to obtain numerical solution can be applied almost to any case, and usually neither simplification nor classification is necessary. Consequently, the problem (3)–(9) was solved numerically.

The finite difference technique [14] was applied for discretization of the mathematical model. We introduced an uniform discrete grid in both x and t directions.

A semi-implicit linear finite difference scheme has been built as a result of the difference approximation of (3), (5), (7), and (8). Since non-linear term related to Michaelis–Menten function contains only one unknown quantity – substrate concentration, then equations (4), (6), and (9) were differenced to a fully implicit scheme. The resulting systems of linear algebraic equations was solved efficiently because of the tridiagonality of the matrices of the systems.

An explicit scheme is easier to program, however, the implicit scheme is more efficient. Although the processing speed of modern computers is high enough to ensure practical use of explicit schemes, the use of the faster implicit scheme well justified because of a large number of simulations, which were carried out in investigation discussed below.

Because of boundary conditions (8) and (9) of the first type on the both borders $x = 0$ and $x = d$ a small step of the grid was required in x direction to have accurate and stable result of computations. Usually an implicit computational scheme does not restrict time increment [14]. However, step size of the grid in time direction is restricted due to the non-linear reaction term in (3), (4) and boundary conditions. An another restriction arises in the case of flow injection analysis, when the boundary condition (8) is a discontinuous function of time. In order to be accurate we employed space step size of $10^{-3}d$ and time step size of 10^{-3} s. For testing of the implicit scheme-based simulator we built also an fully explicit scheme-base simulator. The resulting speed of calculations in case of the explicit scheme was more than 10 times less than in the case

of implicit one. Because of this the implicit scheme-based simulator was employed to investigate the effect of kinetic parameters to biosensor response. The implicit scheme-based simulator runs about 40 s to simulate a 100 s period biosensor action on a PC based Intel Pentium III 750 MHz microprocessor. The software was programmed in C language [20].

In computer simulation, the initial condition $S(x, 0) = \varphi(x)$ was employed instead of (5) to avoid a discontinuity. Here φ is a continuous function: $\varphi(x) = 0$, at $0 \leqslant x \leqslant d - \varepsilon$, φ monotonous increases at $d - \varepsilon < x \leqslant d$, and $\varphi(d) = S_0$. Several different expressions of φ as well as values of small ε were employed. Using the similar technique, the discontinuous boundary condition (8) was also reduced to a continuous one. However, notable difference between solutions was not observed. That is why the equations (5) and (8) is used in simulation discussed bellow.

The current is measured as a response of a biosensor in a physical experiment. The current depends upon the flux of reaction product at the electrode surface, i.e., at border $x = 0$. Consequently, a density i of the current at time t is proportional to the concentration gradient of the product at the surface of the electrode as described by Faraday's law:

$$i(t) = n_e F D_P \frac{\partial P}{\partial x}\bigg|_{x=0}, \tag{10}$$

where n_e is a number of electrons involved in a charge transfer at the electrode surface, and F is Faraday constant, $F \approx 9.65 \times 10^4$ C/mol. Having a numerical solution of the problem (3)–(9), the density of the biosensor current can be calculated easily.

The mathematical model (3)–(9) as well as the numerical solution of the model was evaluated for different values of the maximal enzymatic rate $V_{\max}$. The following values of the parameters were constant in the numerical simulation of all the experiments:

$$D_S = D_P = 3.0 \times 10^{-6} \text{ cm}^2/\text{s}, \quad K_M = 1.0 \times 10^{-7} \text{ mol/cm}^3,$$
$$n_e = 2, \quad d = 0.02 \text{ cm}, \tag{11}$$
$$T_F = 10 \text{ s} \quad \text{(in a case of flow injection analysis only)}.$$

The evolution of the current density as a biosensor response at three values of $V_{\max}$: 10^{-7}, 10^{-8} and 10^{-9} mol/cm^{3}s is presented in figure 1 for both regimes of analyses: batch and flow injection.

Figure 1 shows, that the maximal biosensor current increases with increase of maximal enzymatic rate $V_{\max}$. The time of the maximal biosensor current decreases with the increase of $V_{\max}$. This property is valid for both regimes of analysis: batch and flow injection. In flow injection regime the time of maximal current occurs noticeably later after the time $T_F = 10$ s of analyte removing. For example, in the case when $V_{\max} = 10^{-8}$ mol/cm^{3}s the current starts to decrease with delay of 9 s, i.e., at $t = 19$ s. This delay increases with the decrease of $V_{\max}$.

The biosensor action was simulated also at $V_{\max} = 10^{-6}$ mol/cm^{3}s. However, there was no notable difference between curves of the current at $V_{\max} = 10^{-7}$ and $V_{\max} =$
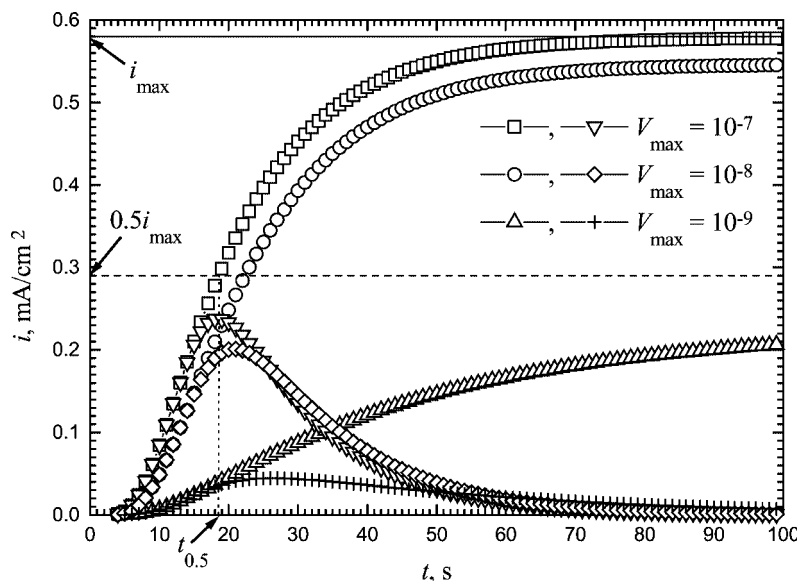
Figure 1. The dynamics of the biosensor current at three maximal enzymatic rates V_{max}: $10^{-7}, 10^{-8}$ and 10^{-9} mol/cm^{3}s in batch ($\square$, O, $\triangle$) and flow injection (∇, $\diamond$, $+$) analysis at substrate concentration of $S_0 = 2 \times 10^{-8}$ mol/cm^3. The solid, dashed, and dot line shows the maximal current, half its and half time its at $V_{\text{max}} = 10^{-7}$ mol/cm^{3}s, respectively.

10^{-6} mol/cm^{3}s. The computer simulation showed, that the relative difference between values of the current density can be noticed when the reaction starts only. This difference exceeds 50% only when $t < 0.6$ s, and it does not exceed 1% when $t > 2.3$ s. This appears in both cases of analysis: batch and flow injection. This effect can be explained by an inequality $10^{-6} \gg K_{\text{M}} = 10^{-7}$. As it is possible to notice in figure 1, even in a case when $V_{\text{max}} = 10^{-8} = 10K_{\text{M}}$ values of the biosensor current differ from the values in another one case when $V_{\text{max}} = 10^{-7} = K_{\text{M}}$ only slightly. Because of this, we accept no values of V_{max} greater than K_{M} in investigation discussed below.

4.   Results and discussion

Using computer simulation we have investigated the dependence of the maximal biosensor current on the concentration of substrate. In the case of batch analysis the maximal biosensor current i_{max} is the steady-state current i_∞. In the computer simulation, every 0.1 s the biosensor response was checked if the steady-state current reached. The calculation was terminated when the relative difference of two last values of the current is less than 10^{-5}%. In flow injection analysis the current function $i(t)$ is not monotonous, therefore the maximal biosensor current i_{max} was calculated by computer simulation until $i(t)$ starts to decrease.

The investigation was carried out at the following values of V_{max}: $10^{-7}, 10^{-8}, 10^{-9}$, 10^{-10}, and 10^{-11} mol/cm^{3}s to get results for a wide range of values of maximal enzy-
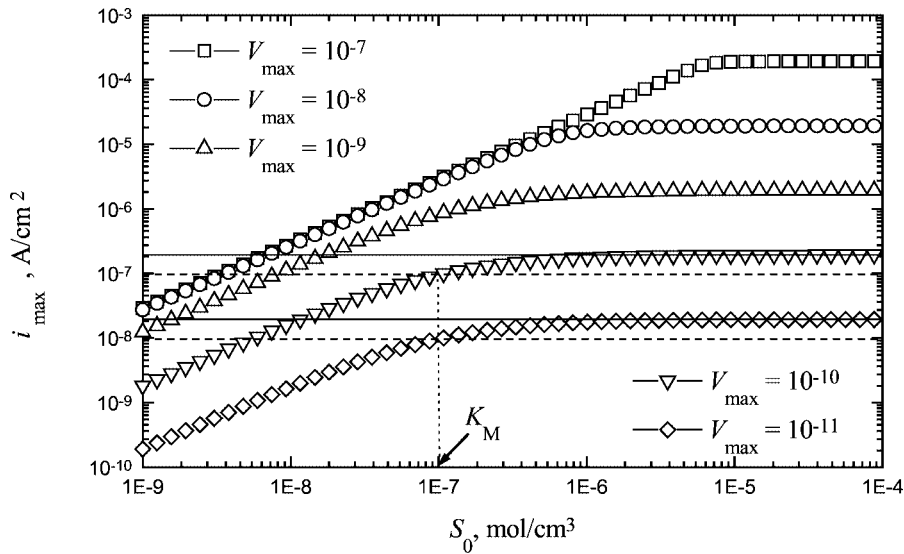
Figure 2. Dependence of the maximal biosensor current on concentration S_0 of the substrate at five maximal enzymatic rates V_{max}: 10^{-7}, 10^{-8}, 10^{-9}, 10^{-10} and 10^{-11} mol/cm^{3}s in batch analysis. The solid and dashed lines show the maximum of maximal current and half its, respectively, at V_{max} of 10^{-11} and 10^{-11} mol/cm^{3}s. The dot line shows Michaelis constant K_M.

matic rate. Results of calculation in the case of batch analysis are depicted in figure 2 while figure 3 presents results for the flow injection analysis. As it is possible to notice, the shape of any curve of the maximal current in batch analysis is very similar to the corresponding one in flow injection analysis. The maximal biosensor current i_{max} is a monotonous increasing function of the substrate concentration at different values of maximal enzymatic rate V_{max} in both regimes of analysis. In both cases of analysis, the maximal current increases only slightly at high concentration of substrate, i.e., $S_0 > 10^{-5}$ mol/cm^3.

Comparing values of the maximal current obtained by different regimes of analysis, we can notice, that the maximal current in batch analysis is greater than the corresponding value in flow injection analysis for all values of S_0 and V_{max}. However, the relative difference of corresponding values of maximal current decreases with increase of substrate concentration. For example, the relative difference between maximal currents in different regimes of analysis is from 2 to 4% at $S_0 = 10^{-4}$ mol/cm^3, for all values of V_{max}. However, the maximal current in batch analysis is 7–25 times greater than corresponding one in flow injection analysis at $S_0 = 10^{-9}$ mol/cm^3. The dependence of maximal current on regime of analysis as well as V_{max} is discussed also below.

The biosensor response is known to be under mass transport control if the enzymatic reaction in the layer of thickness d is faster than the transport process. The concentration of substrate reaches zero inside the enzyme layer at close proximity to $x = d$
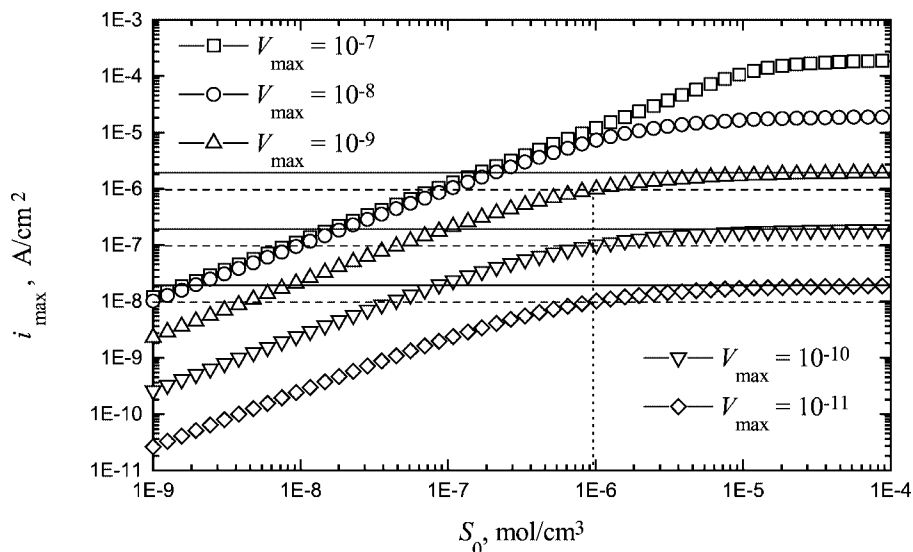
Figure 3. Dependence of maximal biosensor current on concentration S_0 of the substrate at five maximal enzymatic rates V_{max}: 10^{-7}, 10^{-8}, 10^{-9}, 10^{-10} and 10^{-11} mol/cm^{3}s in flow injection analysis. The solid and dashed lines show the maximum of maximal current and half its, respectively, at V_{max} of 10^{-11}, 10^{-10} and 10^{-9} mol/cm^{3}s. The dot line is $S_0 = 9.7 \times 10^{-7}$ mol/cm^3.

when the dimensionless parameter σ is much greater than unity [2], where

$$\sigma = d\sqrt{\frac{V_{max}}{D_S K_M}}. \tag{12}$$

This parameter essentially compares the rate of enzyme reaction (V_{max}/K_M) with diffusion through the enzyme layer (d^2/D_S). If $\sigma < 1$ then enzyme kinetics predominate. The response is under diffusion control if $\sigma > 1$. Since d, D_S, and K_M were constant in our numerical experiments as defined in (11), then $\sigma^2 = 4/3 \times 10^9 V_{max}$. Because of this enzyme kinetics predominate ($\sigma < 1$) when $V_{max} < V_\sigma$, where

$$V_\sigma = \frac{D_S K_M}{d^2} = 0.75 \times 10^{-9} \quad (\text{mol/cm}^3 \text{ s}). \tag{13}$$

The Michaelis constant K_M is known to be the substrate concentration at which the reaction rate is half its maximal value. Figure 2 shows the effect of halving for two values of V_{max}: 10^{-10} and 10^{-11} mol/cm^{3}s at which enzyme kinetics predominate. The maximum of maximal current equals to about 1.93×10^{-7} and 1.93×10^{-8} A/cm^2 at maximal enzymatic rate of 10^{-10} and 10^{-11} mol/cm^{3}s, respectively. Half of the maximum of maximal current is reached at substrate concentration of about $K_M = 10^{-7}$ mol/cm^3 for both values of V_{max}. The relative difference between half of the maximum of maximal current and maximal current at K_M does not exceed 1% at both values of V_{max}. The effect of halving is not valid when the biosensor response is under diffusion control, $V_{max} > V_\sigma$. For example, in the case of $V_{max} = 10^{-9}$ mol/cm^{3}s, the half of the maximum of maximal

current is reached at $S_0 \approx 8.3 \times 10^{-7}$ mol/cm^3 = $8.3 K_M$. It means that the mass transport is significant at maximal enzymatic rate $V_{max} = 10^{-9}$ mol/cm^{3}s and values defined by (11).

We verified if the effect of halving is valid in flow injection analysis exactly like in batch one. The maximum of maximal current equals to about 1.93×10^{-8} A/cm^2 at maximal enzymatic rate of 10^{-11} mol/cm^{3}s (see figure 3). The half of the maximum (9.65×10^{-9} A/cm^2) of maximal current is reached at $S_0 \approx 9.7 \times 10^{-7}$ mol/cm^3 = $9.7 K_M$, which is noticeably far from K_M. However, for two other values of V_{max}: 10^{-10} and 10^{-9} mol/cm^{3}s the half of the maximum of maximal current is reached also at $S_0 \approx 9.7 K_M$. This is not valid for greater values of V_{max}. So, the effect of halving is valid in flow injection analysis in the cases when the biosensor response is under enzyme kinetics control. However, the half of maximum of maximal current differs from Michaelis constant K_M and equals about $9.7 K_M$ at values defined in (11).

The dependence of time moment of occurrence of the maximal current on the substrate concentration was also investigated in both regimes of analysis: batch and flow injection. Since the steady-state time is very sensitive to the error of calculation of maximal current in batch analysis, we investigated the evolution of half of steady-state time [12]. The resultant relative output signal $i^*(t)$ of amperometric biosensor can be expressed as:

$$i^*(t) = \frac{i_\infty - i(t)}{i_\infty}, \qquad i_\infty = \lim_{t \to \infty} i(t), \tag{14}$$

where $i(t)$ is the output current density at time t as defined in (10), i_∞ is the steady-state current.

Let $t_{0.5}$ be the time at which the reaction–diffusion process reaches the medium, called half time of steady-state or, particularly, half of the time moment of occurrence of the maximal current, i.e., $i^*(t_{0.5}) = 0.5$. The half time $t_{0.5}$ of maximal current is presented in figure 1.

Figure 4 shows an effect of substrate concentration S_0 on half time $t_{0.5}$ of maximal biosensor current in batch analysis. Figure 5 shows evolution of time t_{max} of maximal current vs. substrate concentration in flow injection analysis. As it is possible to notice in figures 4 and 5 the corresponding curves of time t_{max} vs. substrate concentration S_0 differs considerably for different regimes of analysis, while figures 2 and 3 show similar behaviour of maximal current. In flow injection regime (figure 5) t_{max} is a monotonous increasing function of S_0 at all values of V_{max}. While figure 4 shows that $t_{0.5}$ is a monotonous decreasing function of S_0 at $V_{max} = 10^{-11}, 10^{-10}$ and 10^{-9} mol/cm^{3}s, and $t_{0.5}$ is even a non-monotonic function at $V_{max} = 10^{-7}$ and 10^{-8} mol/cm^{3}s. This was quite unexpected result. The effect of non-monotony is observed at high maximal enzymatic rate only. As it is possible to notice in figure 4, $t_{0.5}$ gains the maximum at different concentration S_0 of substrate for different values of V_{max}. The half time $t_{0.5}$ of maximal current is reached at $S_0 \approx 6 \times 10^{-6}$ for $V_{max} = 10^{-7}$, while it appears at $S_0 \approx 5 \times 10^{-7}$ mol/cm^3 for $V_{max} = 10^{-8}$ mol/cm^{3}s. Additional calculation showed that the curve of half time $t_{0.5}$ vs. S_0 monotonously decreases for all values of V_{max}
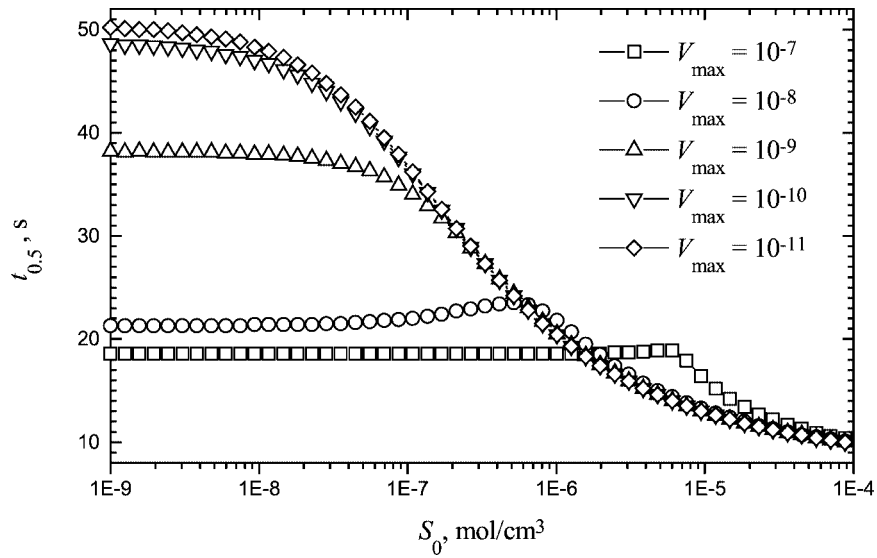
Figure 4. Dependence of half time of the maximal biosensor current on the concentration S_0 of substrate at five maximal enzymatic rates V_{max}: 10^{-7}, 10^{-8}, 10^{-9}, 10^{-10} and 10^{-11} mol/cm^{3}s in batch analysis.
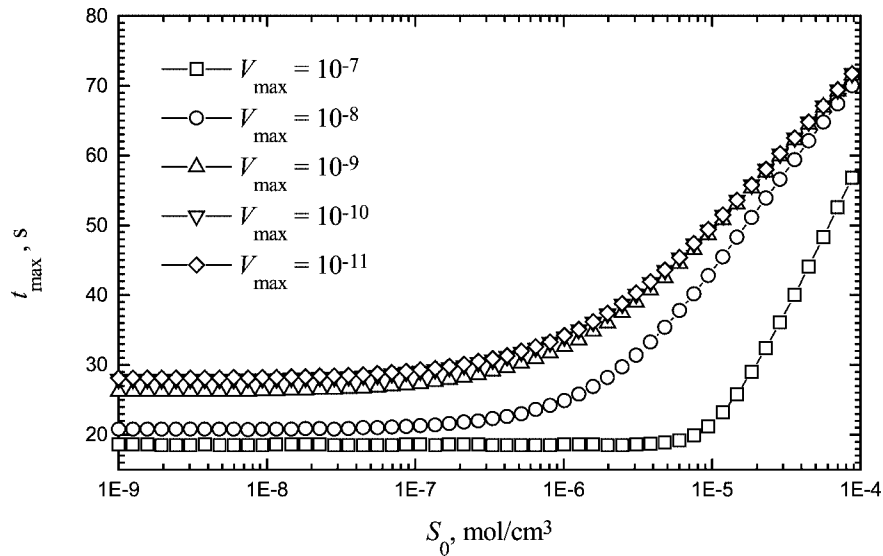

Figure 5. Dependence of time of maximal biosensor current on concentration S_0 of the substrate at five maximal enzymatic rates V_{max}: 10^{-7}, 10^{-8}, 10^{-9}, 10^{-10} and 10^{-11} mol/cm^{3}s in flow injection analysis.

greater than about 10^{-9} mol/cm^{3}s. Let us notice that this value correlates with a value of V_σ (see (13)) at which the diffusion begins to predominate in the biosensor response. We conclude that non-monotonous evolution of the half time $t_{0.5}$ of maximal biosensor
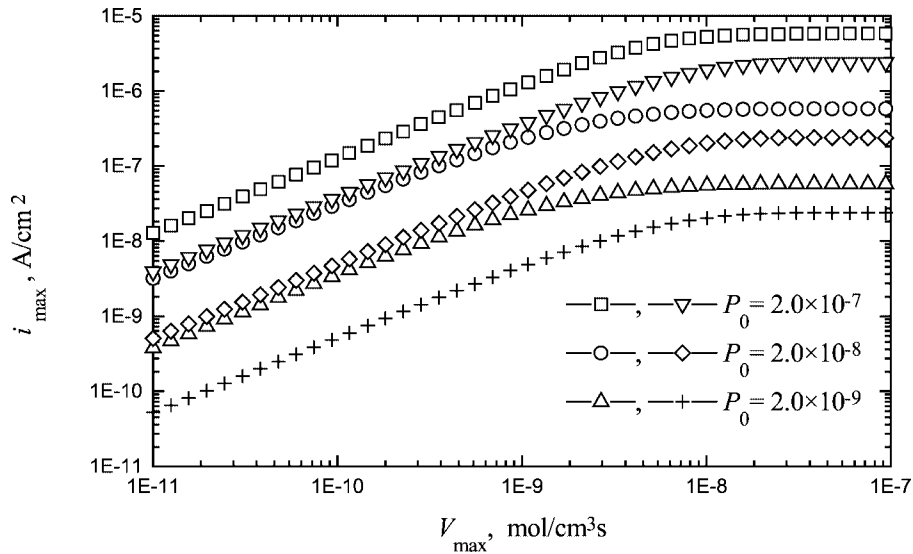
Figure 6. The maximal biosensor current versus maximal enzymatic rate V_{max} at three concentrations S_0 of substrate: 2.0×10^{-9}, 2.0×10^{-8} and 2.0×10^{-7} mol/cm^3 in batch ($\square$, $\bigcirc$, $\triangle$) and flow injection (∇, $\diamond$, $+$) analysis.

current versus substrate concentration can be observed when the biosensor response is under diffusion control.

Figure 4 shows also that half time $t_{0.5}$ of maximal current almost does not depend on the maximal enzymatic rate V_{max} at very high concentrations S_0 of substrate ($S_0 > \sim 5.0 \times 10^{-5}$ mol/cm^3) in batch analysis. Particularly, values of $t_{0.5}$ differs by less than 5% only at $S_0 = 10^{-4}$ mol/cm^3.

Figure 5 shows the considerable increase of time t_{max} of maximal current vs. substrate concentration S_0 at high values of S_0 only in flow injection analysis. This can be explained by sufficient supply of the substrate after the time T_F (see (8)) when the substrate was removed from solution. The more substrate penetrates into the enzyme layer until time T_F, the longer reaction performs. The time of maximal current increases very weakly vs. S_0 at low values of S_0 ($S_0 < \sim 5.0 \times 10^{-7}$ mol/cm^3).

We have investigated also the dependence of time of the maximal biosensor current on the maximal enzymatic rate V_{max} at different concentration S_0 of the substrate. Results of computer simulation are depicted in figure 6 and 7 at three concentrations S_0: $2 \times 10^{-7}, 2 \times 10^{-8}$ and 2×10^{-9} mol/cm^3 in both regimes of analysis. Figure 6 shows that the maximal current is higher in batch analysis than an another one in flow injection analysis at full range of investigated maximal enzymatic rates ($10^{-11} \leqslant V_{max} \leqslant 10^{-7}$ mol/cm^{3}s) and concentration $S_0 \in \{2 \times 10^{-7}, 2 \times 10^{-8}, 2 \times 10^{-9}$ mol/cm$^3\}$. The maximal current in flow injection analysis is up to 10 times less than the maximal current in batch analysis. This was also discussed above also for wider range of S_0. Let us notice, that the shape of the curve of maximal current is similar in all the cases including results presented in figures 2 and 3.
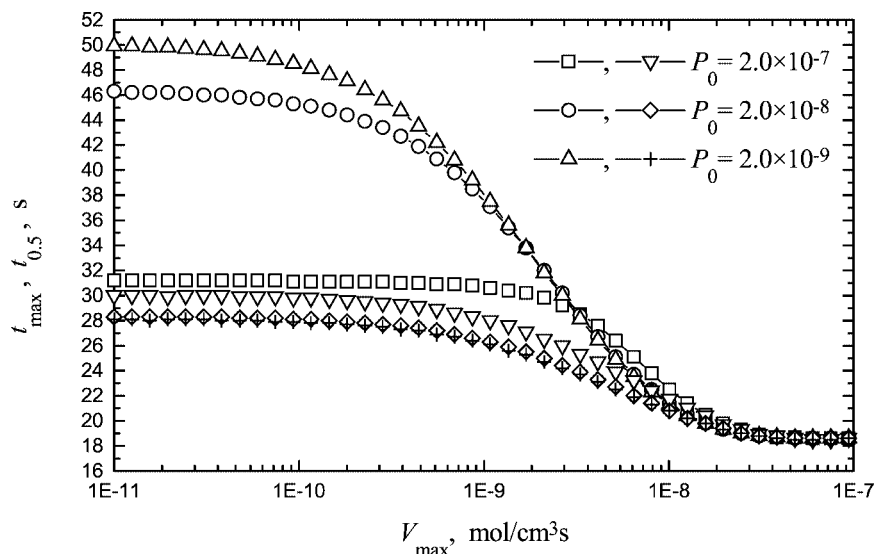
Figure 7. Time (in batch analysis) and half time (in flow injection analysis) of the maximal biosensor current versus maximal enzymatic rate V_{max} at three concentrations S_0 of substrate: 2.0×10^{-9}, 2.0×10^{-8} and 2.0×10^{-7} mol/cm^3 in batch ($\square$, $\bigcirc$, $\triangle$) and flow injection (∇, $\diamond$, $+$) analysis.

Figure 7 shows that time of maximal current decreases with increase of maximal enzymatic rate V_{max} in both regimes of analysis. It was unexpected to see that time t_{max} of maximal current in batch analysis and half time $t_{0.5}$ in flow injection analysis differs slightly only at high values of V_{max}. E.g., $t_{max} = 18.5$, $t_{0.5} = 18.6$ s at $V_{max} = 10^{-7}$ mol/cm^{3}s for all three values of S_0. t_{max} varies from 20.8 to 21.7 and $t_{0.5}$ from 21.3 to 22.5 s at $V_{max} = 10^{-8}$ mol/cm^{3}s. Variation of t_{max} as well as $t_{0.5}$ increases with decrease of V_{max}. However, maximal time in batch analysis ($t_{0.5}$) varies much more that another one in flow injection analysis (t_{max}). Particularly, there is no notable difference between curves of t_{max} at $S_0 = 2 \times 10^{-9}$ and $S_0 = 2 \times 10^{-8}$ mol/cm^3. The maximal difference between these two curves is about 0.3 s only.

5.   Conclusion

The mathematical model (3)–(9) of amperometric biosensor operation can be successfully used to investigate the kinetic regularities of biosensors in both regimes of analysis: batch and flow injection.

A non-monotonous evolution of the half time of the maximal biosensor current versus substrate concentration is observed when the biosensor response is under diffusion control in batch analysis. At the beginning, the half time increases with increase of substrate concentration. The increase of half time up to 10% was observed in computer simulation. Later the half time begins to decrease (see figure 4).

The effect of halving of maximal current is valid in flow injection analysis (figure 3) as well as in batch analysis (figure 2) in the cases when the biosensor response is under

enzyme kinetics control. However, in the flow injection analysis, the half of maximum of maximal current differs from Michaelis constant K_M and equals about $9.7K_M$ at values defined in (11).

Acknowledgement

References

[1] L.C. Clarc and C. Loys, Ann. N.Y. Acad. Sci. 102 (1962) 29.
[2] F. Scheller and F. Schubert, *Biosensors*, Vol. 7 (Elsevier, Amsterdam, 1992).
[3] A. Chaubey and B.D. Malhotra, Biosens. Biolectron. 17 (2002) 441.
[4] E.J. Calvo and C. Danilovich, J. Braz. Chem. Soc. 8 (1997) 563.
[5] C.D. Mell and J.T. Maloy, Anal. Chem. 47 (1975) 299.
[6] C.D. Mell and J.T. Maloy, Anal. Chem. 48 (1976) 1597.
[7] J.J. Kulys, V.V. Sorochinskii and R.A. Vidziunaite, Biosensors 2 (1986) 135.
[8] T. Schulmeister, Selective Electrode Rev. 12 (1990) 260.
[9] V.V. Sorochinskii and B.I. Kurganov, Biosens. Bioelectron. 11 (1996) 225.
[10] K. Yokoyama and Y. Kayanuma, Anal. Chem. 70 (1998) 3368.
[11] R. Baronas, F. Ivanauskas and J. Kulys, J. Math. Chem. 25 (1999) 245.
[12] J. Crank, *The Mathematics of Diffusion*, 2nd ed. (Clarendon Press, Oxford, 1975).
[13] J. Ruzicka and E.H. Hansen, *Flow Injection Analysis* (Wiley, New York, 1988).
[14] W.F. Ames, *Numerical Methods for Partial Differential Equations*, 2nd ed. (Academic Press, New York, 1977).
[15] D. Britz, *Digital Simulation in Electrochemistry*, 2nd ed. (Springer, Berlin, 1988).
[16] P.N. Bartlett and K.F.E. Pratt, J. Electroanal. Chem. 397 (1995) 61.
[17] P.N. Bartlett and K.F.E. Pratt, Biosens. Bioelectron. 8 (1993) 451.
[18] B. Lavine, Anal. Chem. 70 (1998) 209R.
[19] T. Artursson, T. Eklöv, I. Lundström, P. Mårtenson, M. Sjöström and M. Holmberg, J. Chemometrics 14 (2000) 711.
[20] S.A. Teukolsky, W.T. Vetterling and B.P. Flannery, *Numerical Recipes in C: The Art of Scientific Computing* (William H. Press, 1993).